Beni-Suef University Journal of Basic and Applied Sciences

RESEARCH

Open Access

Improved oral bioavailability of poorly water-soluble vorinostat by self-microemulsifying drug delivery system

Ashok Kumar Janakiraman[1*], Tahani Islam[1], Kai Bin Liew[2], Manogaran Elumalai[1] and J. C. Hanish Singh[3]

Abstract

Background: Vorinostat is a histone deacetylase inhibitor suberoylanilide hydroxamic acid (SAHA) with anticancer properties. However, it is plagued by low water solubility, low permeability (BCS class IV drug), and suboptimal pharmacokinetics. The purpose of the present study was to develop a self-microemulsifying drug delivery system (SMEDDS) to enhance the oral bioavailability of vorinostat. Capryol 90, labrasol, and polyethylene glycol (PEG 400) were selected as oil phase, surfactant, and co-surfactant, respectively. The vorinostat self-microemulsifying drug delivery systems were tested for self-microemulsifying time, phase separation, effect of pH, droplet size, zeta potential, dilution study, Fourier-transform infrared (FT-IR) spectroscopy analysis, and field emission scanning electron microscopy (FESEM). A rat model in vivo pharmacokinetic study was conducted for the optimized formulation against vorinostat pure drug powder.

Results: The results from the characterization studies showed that the optimized formulation (F7) self-microemulsification time was 1.4 ± 0.05 min and no precipitation or phase separation was observed. The mean droplet size, polydispersity index (PDI), and zeta potential of the optimized formulation (F7) were found to be 272.9 ± 82.7 nm, 0.415, and -57.2 mV, respectively. The pharmacokinetic parameters of the optimized formulation (F7) showed a 1.6-fold increase in maximum concentration (C_{max}) and a 3.6-fold increase in area under the curve ($AUC_{(0-\infty)}$), in comparison with pure drug in suspension.

Conclusions: The findings suggest that SMEDDS formulation could be an effective method for increasing the oral bioavailability of vorinostat, which is poorly water soluble.

Keywords: Vorinostat, Self-microemulsion, Surfactant, Interface, In vivo pharmacokinetic study, Oral bioavailability

1 Background

Oral route remains the most convenient and popular path of drug administration to this day. However, it has been reported that 40% of drug compounds have inadequate aqueous solubility. Developing dose proportionality and recovering intra- and inter-subject inconsistency of drugs in blood plasma concentration remain a great challenge [1, 2]. According to the biopharmaceutical classification system (BCS), these drugs are classified as BCS class II drugs with minimal aqueous solubility and excessive permeability, and BCS class IV drugs with poor aqueous solubility and low level of permeability. Dissolution and bioavailability are major areas of concern for this group of drugs. Recently, drug carrier systems have been used to overcome poor aqueous solubility to improve dissolution rate and bioavailability. Different types of formulation techniques have been developed to enhance the oral bioavailability of poorly soluble drugs. These include solid dispersions, permeation enhancers, complexation with cyclodextrins, emulsions, liposomes, lipid-based

*Correspondence: akpharm@gmail.com; ashok@ucsiuniversity.edu.my

[1] Faculty of Pharmaceutical Sciences, UCSI University, 56000 Cheras, Kuala Lumpur, Malaysia
Full list of author information is available at the end of the article

formulations, micronization, and nanoparticles [3–5]. These approaches have a few challenges, such as the need for specialized equipment, complicated manufacturing processes, longer processing times, and regulatory complexity.

Self-microemulsifying drug delivery systems (SMEDDSs) are promising approaches to enhance the solubility of poorly soluble drugs and have several advantages; oil droplet size of the dispersion ranged between 200 nm and 5 μm [6]. SMEDDS is an isotropic mixture of drug, oil, surfactant(s), and co-surfactant(s) which spreads rapidly in the gastrointestinal tract (GIT) upon dilution with gastric juice and spontaneously forms microemulsions [7, 8]. The particle size of the microemulsion is micro to nano, in contrast with ordinary emulsions. Microemulsions are thermodynamically stable once interfacial tension between two immiscible phases reduces to zero and the spontaneous formation of microemulsion produces negative free energy [9]. The small droplet size of microemulsion helps to improve absorption and can increase the interfacial surface area for drug release.

Vorinostat is a histone deacetylase (HDAC) inhibitor. Restoration of normal acetylation apoptosis cell cycle arrest may occur due to the presence of anticancer properties in HDAC inhibitor vorinostat [10]. However, vorinostat is plagued by low water solubility (0.2 mg/mL), low permeability, and poor pharmacokinetics, which results in difficulty for parenteral formulation [11, 12]. Vorinostat is also plagued by suboptimal pharmacokinetics including low bioavailability (43% for humans and 11% for rats), extensive serum clearance, and a short elimination half-life of approximately 2 h in both animal and human studies [13–17]. Much of the short half-life and limited overall exposure of vorinostat is related to its rapid metabolism, which is its predominate route of elimination. Vorinostat is metabolized via two metabolic pathways including glucuronidation and hydrolysis followed by β-oxidation. These pathways produce two inactive metabolites, a vorinostat glucuronide and a vorinostat hydrolysis metabolite, 4-anilino-4-oxobutanoic acid, both of which are excreted in the urine [18]. Therefore, considering its medical importance several researchers [19–21] have developed novel formulations of vorinostat for both oral and parenteral administrations that improve solubility and the overall disposition profile of vorinostat. However, still there is a need of developing an effective dosage form for enhancing the bioavailability of vorinostat.

Considering the above-stated problems, the aim of the present study was designed to develop a SMEDDS to enhance the oral bioavailability of a hydrophobic drug vorinostat. In this research, vorinostat SMEDDS formulations were developed, and various physicochemical characteristics were evaluated along with in vivo pharmacokinetic studies. SMEDDS is a physically stable formulation that may bypass the hepatic first-pass metabolism and reduce pre-systemic clearance in the gastrointestinal (GI) mucosa. Hence, the presence of lipid in the formulation serves to enhance the bioavailability of vorinostat.

2 Methods

2.1 Solubility studies

Excessive amount of vorinostat (about 10 mg) was added into each five mL vehicle in a screw cap vial and mixed continuously for 1 min using a vortex mixer. The vial was then kept in a water bath at 40 °C ± 0.5 °C for 15 min to facilitate solubilization and mixed again for 1 min. Afterward, the mixtures were shaken with a shaker incubator at 37 °C ± 0.5 °C for 48 h at 200 rpm. After reaching equilibrium, the mixtures were centrifuged at 3000 rpm for 5 min to remove the excess (undissolved) vorinostat. Drug content was determined by a UV–visible spectrophotometer at 242 nm [22]. All samples were triplicated to determine the standard deviation.

2.2 Construction of pseudoternary phase diagram

A pseudoternary phase diagram was constructed at room temperature to identify the self-microemulsifying regions through water titration and to determine the concentration of components for the accessible range of SMEDDS. Pseudoternary phase diagrams were constructed based on the selection of the most suitable surfactant and co-surfactant. The mixtures of lipids, surfactant, and co-surfactant were serially titrated by water and mixed with a vortex mixer, which were then characterized through visual observation [23]. This was done using CHEMIX School 7.0 software to construct pseudoternary phase diagrams. Each of the diagram represents an apex of the triangle, and the total was kept at 100%. To identify self-microemulsion regions, a series of pseudoternary phase diagrams were plotted and through direct observation, the size of emulsion region among the diagrams was compared [24].

Mixtures of oil and surfactant/co-surfactant in preferred ratios were diluted with drops of water [25]. Based on the drug solubility study, selected oil phase, surfactant, and co-surfactant were used for the phase diagram study using ultra-pure water as an aqueous phase. Surfactant and co-surfactant were mixed using a vortex mixer in different volume ratios (1:1, 2:1, 3:1, 1:3, 2:3, and 3:2) in glass vials and named S_{mix}. The S_{mix} ratio was chosen in increasing the concentration of surfactant on the subject of co-surfactant and increasing the concentration of co-surfactant on the subject of surfactant. The mixture

of oil and S_{mix} was in various volume ratios, from 1:9 to 9:1 (1:9, 2:8, 3:7, 4:6, 5:5, 6:4, 7:3, 8:2, and 9:1), and carried out in different glass vials at room temperature. Through slow titration of the oil phase, each ratio of S_{mix} was performed individually by adding ultra-pure water using a micropipette, which was then mixed with a vortex mixer until it turned turbid [26, 27]. The sample was considered a microemulsion if a clear and transparent mixture was obtained after stirring. All studies were triplicated, and similar observations were made.

2.3 Preparation of vorinostat self-microemulsion

Three components of self-microemulsification system, viz. oil, surfactant, and co-surfactant ratios, were identified by employing the pseudoternary phase diagram. Vorinostat (10 mg) was dissolved in selected oils into a screw cap vial and mixed with a vortex mixer (Lambert 3000, Copens Scientifics (M) Sdn. Bhd., Malaysia) for 20 min. Surfactant and co-surfactant were then added, and again, the components were mixed for 20 min. After that, the mixture was heated in a water bath at 30 °C ± 0.5 °C for 30 min [28]. The formulation was sonicated in an ultrasonic bath and stored at room temperature until it was used in subsequent studies.

2.4 Self-microemulsification time and phase separation study

The self-microemulsification time of SMEDDS was assessed visually. Visual assessment was performed by adding drops of SMEDDS (100 µL) into 100 mL of distilled water in a glass beaker at 37 ± 5 °C. The contents were gently stirred with a magnetic stirrer at 100 rpm [29]. The time taken for emulsion formation (until a homogenous system was obtained) was observed and recorded as self-microemulsification time.

Prepared SMEDDS (50 µL) was added into a glass test tube containing 5 mL ultra-pure water at 37 ± 5 °C and mixed with a vortex mixer for 1 min. Visual assessment was performed from the start to 12 h and recorded. The resulting mixture was stored for a period of 24 h and observed for phase separation and precipitation of the drug [30].

2.5 Effect of pH in different media

The apparent pH of the prepared formulations was measured using a calibrated pH meter with glass electrode at room temperature. For the effect of pH, SMEDDS formulations were subjected to (1:1000) in ultra-pure water with 0.1 M HCl and pH 6.8 phosphate buffer in a glass beaker [28].

2.6 Dilution test

The emulsions were further studied in a dilution test for visual assessment of appearance (clear, transparent, opalescent, or bluish white). The dilution test was carried out by diluting the prepared SMEDDS which was subjected to 1:50, 1:100, 1:500, and 1:1000 ratios in ultra-pure water with 0.1 N HCl and phosphate buffer (pH 6.8). The diluted self-microemulsions were stored for 24 h and observed for any sign of phase separation or drug precipitation [31].

2.7 Freeze–thaw stability

The stability of the vorinostat SMEDDS formulations was determined through freeze–thaw cycles. Approximately, 1 mL of SMEDDS formulations was placed into Eppendorf tubes and a total of four complete freeze–thaw cycles were performed. Each cycle took about 24 h at 20 °C and 40 °C, and visual observation was performed after each cycle. After completion of four freeze–thaw cycles, the formulations were centrifuged at 3000 rpm for 5 min and observed for any phase separation or precipitation of the drug [32].

2.8 Particle size analysis and zeta potential

The average droplet size, PDI, and electrophoretic mobility (zeta potential) were measured by photon correlation spectroscopy using a Malvern Zetasizer (Nano ZS90; Malvern Instruments) at 25 °C. The samples were kept in a polystyrene cuvette; the readings were noted at 90-degree fixed angles and diluted suitably using Millipore water pH 5.5 [33, 34].

2.9 Viscosity analysis

Small quantities (five to six drops) of each formulation were added manually to the plate, and the viscosity of formulations was determined with the help of Haake RheoWin RotoVisco RV1 (Thermo Scientific, Germany) viscometer at 25 ± 1 °C, with a uniform acceleration of the plate from zero to 300 s^{-1} within 3 min followed by decelerated uniformity back to zero within 3 min. The viscosity was triplicated to determine the standard deviation.

2.10 Fourier-transform infrared (FT-IR) spectroscopy analysis

An FT-IR Nicolet iS5 (Thermo Fischer Scientific, USA) was used to determine the drug–excipient compatibility. The drug (vorinostat) and optimized formulation (F7) IR spectra were recorded using infrared spectra. A small amount of each sample was put directly on the diamond crystal plates, and 4 scans were taken at a

resolution of 1 cm^{-1} from a frequency range of 4000–400 cm^{-1} for each sample [35].

2.11 Field emission scanning electron microscopy (FESEM)

A FESEM (Quanta 250, Bruker) was used to observe the morphologies of vorinostat SMEDDS. Prior to the FESEM analysis, one drop of SMEDDS was poured onto a carbon tape and dried at room temperature. The dried sample was sputter-coated using a gold target for a short time (approximately 10–15 s) under a high vacuum. High-resolution images were taken at 20 kV and accelerating voltage at 280× magnification value [36].

2.12 In vitro dissolution studies

The in vitro dissolution study of vorinostat SMEDDS was performed using USP type II (paddle), and the pure drug was carried out using USP type I (basket) dissolution apparatus (Electro Lab, India). The optimized vorinostat SMEDDS (F7) and pure drug were filled individually in hard gelatine capsule shells. Each capsule was placed into a dissolution vessel containing 900 mL of phosphate buffer (pH 6.8) at 37 ± 0.5 °C and rotated at 50 rpm for both basket and paddle [37, 38]. Aliquot five mL of samples was withdrawn after 5, 10, 15, 30, 45, 60, 90, and 120 min, respectively, and replaced by the same volume of fresh medium at 37 °C ± 0.5 °C. The samples were filtered through a 0.45-µm disk filter, and the amount of vorinostat released was determined spectrophotometrically at 242 nm. Each experiment was carried out triplicated. The drug release was fitted to various kinetic models.

2.13 In vivo pharmacokinetic studies

Male Sprague Dawley rats weighing between 200 and 250 g were used for the in vivo pharmacokinetic study. All animal experiments and the procedures involved were adhered to standard protocol complying with the European Union guidelines (directive 2010/63/EU) [39] followed by the institutional animal ethics committee (IAEC), KPJ Healthcare University College (KPJUC), Nilai, Malaysia. The experimental protocol was approved, and consent for animal experimentation was obtained from IAEC (Ref. No. KPJUC/RMC/EC/2018/132). Inbreed animals in KPJUC were acclimatization for one week before the experiment. The animals were kept under standard laboratory conditions at a temperature of 25 °C ± 2 °C with relative humidity of 55 ± 5% and 12-h of light–dark cycles. All the rats were fasted overnight with free access to water prior to the experiment [40]. Effective sample size calculation was performed by power analysis at a 95% confidence interval and considered the minimum number of animals [41]. A total of 12 animals were divided into two groups of each six animals which were used in this experimental protocol. Group I (6 animals) was treated with SMEEDS (F7, vorinostat-loaded SMEDDS 10 mg/kg), and group II (6 animals) was treated with pure active pharmaceutical ingredient (Vorinostat in suspension, 10 mg/kg). Vorinostat-loaded SMEDDS and vorinostat drug in suspension (pure drug) were administrated to the rats using oral gavage. Blood samples (0.2 mL) were collected retro-orbital sinus puncture at predetermined times (0.5, 1, 2, 4, 6, and 8 h) after administration under light ether anesthesia (inhalation), and care was taken as per IAEC guidelines. Plasma samples were separated immediately by centrifugation at 4000 rpm for 5 min and stored at − 20 °C until further analysis [42]. After the experimental study, the animals were monitored for 2 weeks for recovery and monitored for chemical safety for sustainability [43].

Sample analysis The analysis was performed using the high-performance liquid chromatography (HPLC) (Waters Corporation, Milford, USA) which consisted of an isocratic pump 1515, dual absorbance detector 2487, and refractometer 2410 with breeze software. The column used was Ultisil, XB-C18 (0.5 µm, 0.46 X 250 mm, Welch Materials) which was maintained at room temperature. Methanol and phosphate-buffered solution (PBS) (60:40 v/v; PBS pH 3.5 adjusted with phosphoric acid) were used as the mobile phase. The mobile phase was filtered through a 0.45-µm membrane filter and degassed in an ultrasonic bath for 10 min before use. The flow rate of the mobile phase was optimized at 0.9 mL/min. The injection volume was 10 µL, and the chromatographic run time was adjusted to 10 min. The effluent was monitored at a UV absorption wavelength of 245 nm for the analysis of the drug. The calibration curve of vorinostat in plasma was constructed over a range of 50 to 800 ng/mL. Blank plasma samples were spiked with a stock solution, and protein precipitation was carried out with the addition of methanol. 200 µL of methanol was mixed with 100 µL of blank plasma sample spiked with drug and mixed with a vortex mixer for 30 s. The separation of precipitation from the organic phase was achieved by centrifugation at 13,000 rpm. The supernatant was collected and filtered using a 0.45-µm disk filter, and 10 µL was injected into the HPLC system. The sample treatment followed the same protein deproteinization procedure without any drug solution.

The pharmacokinetic parameters, including the area under the plasma drug concentration–time curve ($AUC_{0-\infty}$), time to reach the maximum plasma drug concentration (T_{max}), maximum plasma drug concentration (C_{max}), and the elimination of half-life ($t_{1/2}$), were calculated by non-compartmental modeling using PKSolver 2.0 (Excel add-in program on Microsoft EXCEL). All values were expressed as the mean ± standard deviation (SD).

2.14 Statistical analysis

The statistical analysis of in vitro dissolution studies was performed using Student's *t* test, and pharmacokinetic parameters (in vivo) of different groups were analyzed using a one-way ANOVA followed by Tukey–Kramer's multiple comparisons test at a significance level of $p < 0.05$ using IBM SPSS statistical (SPSS version 20) software [44].

3 Results

Drug solubility was screened in various oil, surfactant, and co-surfactant in self-microemulsifying formulation. The solubility data of vorinostat in various vehicles are provided in Table 1. Vorinostat showed the highest solubility in capryol 90 (1.666 ± 0.058 mg/mL) followed by oleic acid (1.268 ± 0.142 mg/mL). Surfactant, span 20, and labrasol (medium-length alkyl chain surfactant) showed high solubility of 1.734 ± 0.145 mg/mL and 1.612 ± 0.128 mg/mL, respectively. Among the different co-surfactants used in this study, PEG 400 exhibited maximum solubility (2.169 ± 0.138 mg/mL) for vorinostat.

In pseudoternary phase diagram study, oleic acid, labrasol, and PEG 400 (series 1) formed a small emulsion area as compared to capryol 90, labrasol, and PEG 400 (series 2) and capryol 90, span 20, and PEG 400 (series 3). It was observed that series 2 showed small increase in emulsion area as compared to series 1 and 3. The emulsion area was larger for labrasol compared to span 20. Capryol 90 with labrasol showed a higher emulsion area (Fig. 1a) than oleic acid and labrasol. Furthermore, in series 2, as the concentration of surfactant (S_{mix} 3:1) increased, the solubilization of oil slightly decreased (Fig. 1b). An additional pseudoternary phase diagram file shows in more detail series1, series 2, and series 3 (Additional file 1).

The recorded self-microemulsification times of vorinostat-loaded formulations are represented in Table 2.

Table 1 Solubility of vorinostat in oils, surfactants, and co-surfactants

Vehicle	Function in SMEDDS	Avg. solubility (mg/mL)*
Oleic acid	Oil	1.268 ± 0.142
Castor oil	Oil	0.448 ± 0.002
Capryol 90	Oil	1.666 ± 0.058
Tween 20	Surfactant	1.337 ± 0.014
Span 20	Surfactant	1.734 ± 0.145
Labrasol	Surfactant	1.612 ± 0.128
1,2 Propylene glycol	Co-surfactant	1.865 ± 0.012
Polyethylene glycol 200	Co-surfactant	1.840 ± 0.026
Polyethylene glycol 400	Co-surfactant	2.169 ± 0.138

*Each value represents the mean ± SD ($n = 3$)

From the results obtained, all the tested formulations of vorinostat SMEDDS found self-microemulsification within 0.88 ± 0.06 (53 ± 4 s) to 2.58 ± 0.51 min.

The pH of selected vorinostat-loaded SMEDDS in different media ranged from 1.20 ± 0.105 to 6.85 ± 0.122 is presented in Table 3.

All investigated droplet size of the formulations, PDI, and zeta potential values are presented in Table 4. The particle size distribution of selected formulations was 272.9 ± 82.7 to 677.8 ± 235.2 nm, and the high percentage of SD observed in the droplet size of the emulsion may be due to the reduction in the steric repulsion between droplets. An additional file shows the particle size distribution and PDI of vorinostat loaded SMEDDS (F7) (Additional file 2). An additional file shows the zeta potential of vorinostat loaded SMEDDS (F7) (Additional file 3).

FT-IR spectra of pure vorinostat and vorinostat-loaded SMEDD (F7) are presented in Fig. 2. The FT-IR spectra of vorinostat displayed bands at 3195.15 and 1547.35 cm^{-1} due to N–H stretching and N–H bending, 2934.52 and 2861.65 cm^{-1} due to C–H stretching, at 1654.90 cm^{-1} due to C=O stretching, at 1597 cm^{-1} due to C=C stretching. The spectra also showed bands at 1130.93 to 1058.96 cm^{-1} due to C–O stretching. The FT-IR spectrum of SMEDDS (F7) exhibited characteristic bands consistent with the molecular structure of vorinostat at 3444.01 cm^{-1} due to N–H stretch, at 2922.91 and 2858.85 cm^{-1} due to C=H stretching, and at 1101.07 cm^{-1} range peak due to C–O stretching. An additional FT-IR file shows spectra of vorinostat with capryol 90, labrasol, and PEG 400 (Additional file 4).

The morphology of the optimized vorinostat-loaded self-microemulsion was determined using FESEM depicted in Fig. 3. Droplets were visualized for the detection of morphology like the size and shape of the droplets. The shape of the vorinostat-loaded self-microemulsion (F7) with capryol 90, labrasol, and PEG mixture was found to be spherical.

A comparison of the in vitro drug release between pure drug (vorinostat powder) and vorinostat-loaded optimized SMEDDS formulation (F7) is depicted in Fig. 4. The in vitro drug release profile of pure drug and optimized SMEDDS formulation was 17% and 95%, respectively, after 120 min. The drug release was fitted to various kinetic models such as zero order, first order, and Higuchi whose r^2 value was found as 0.7913, 0.7697, and 0.895, respectively. The Peppa's plot shows the r^2 value and n value of 0.8757 and 2.605.

The plasma concentration of vorinostat versus the time profiles of group I and group II is shown in Fig. 5, and pharmacokinetic parameters are presented in Table 5. The plasma concentration profile of vorinostat

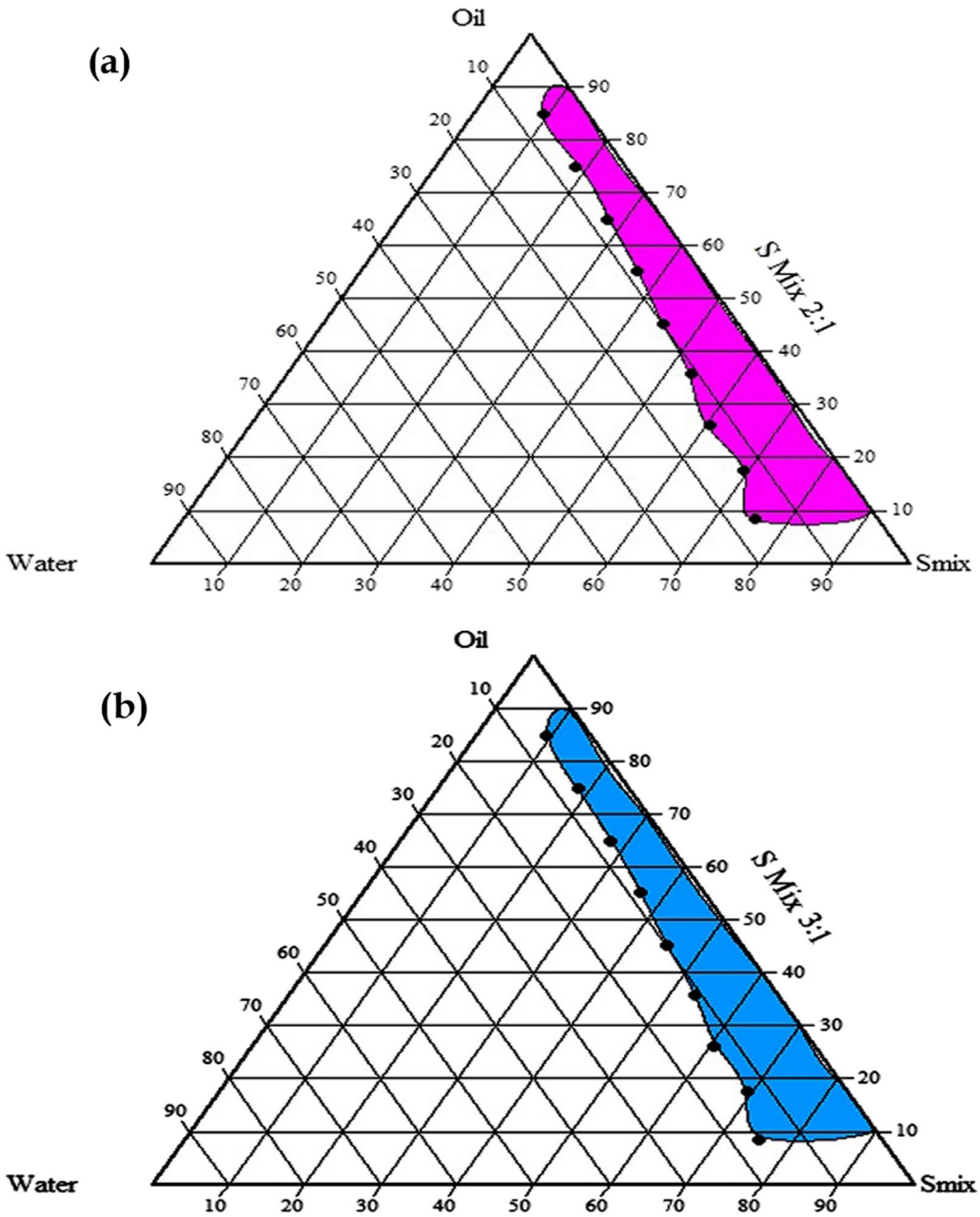

Fig. 1 Pseudoternary phase diagram of **a** capryol 90 with labrasol S_{mix} 2:1emulsion area, **b** capryol 90 with labrasol S_{mix} 3:1 emulsion area pseudoternary phase diagram (S_{mix} 2:1)

for prepared SMEDDS (10 mg/kg) represented a greater improvement of drug absorption than a pure drug in suspension.

4 Discussion

Identification of suitable excipients for SMEDDS is a crucial factor to obtain the highest solubility capacity with optimum drug loading [22, 45]. Hence, capryol 90 and oleic acid were chosen as oil phases for vorinostat SMEDDS formulation. Capryol 90 is a common penetration enhancer, which may be attributed to the medium chain length (eight carbons) and its amphiphilic nature. Researchers [46, 47] suggested that capryol could provide an optimal SMEDDS formulation resulting in the improvement of drug loading and the formation of the spontaneous fine emulsion. On the other hand, oleic acid

Table 2 Self-emulsification time, appearance, and phase separation of vorinostat-loaded SMEDDS

Formulation code	Self-emulsification time (min)*	Appearance	Phase separation for 24 h[#]
F1	1.95 ± 0.26	Bluish white	NPS
F2	1.38 ± 0.12	Bluish white	NPS
F3	2.58 ± 0.51	Bluish white	NPS
F4	2.27 ± 0.02	Bluish white	NPS
F5	–	Large oil droplets	NPS
F6	1.08 ± 0.01	Bluish white	NPS
F7	1.47 ± 0.05	Clear and transparent	NPS
F8	1.18 ± 0.01	Clear and transparent	NPS
F9	–	Large oil droplets	NPS
F10	–	Large oil droplets	NPS
F11	1.30 ± 0.05	Clear and transparent	NPS
F12	0.88 ± 0.06 (53 ± 4 s)	Clear and transparent	NPS

Each value represents the mean ± SD ($n = 3$)

*Self-emulsification time (s)

[#] *NPS* no phase separation

Table 3 The pH of vorinostat-loaded SMEDDS in different media

Media	pH	SMEDDS in media (1:1000)			
		F7	F8	F11	F12
UPW	7.7	5.37 ± 0.050	5.21 ± 0.049	5.40 ± 0.034	5.35 ± 0.035
0.1 M HCl	1.15	1.20 ± 0.105	1.22 ± 0.030	1.21 ± 0.030	1.21 ± 0.061
PB	6.8	6.70 ± 0.120	6.85 ± 0.122	6.78 ± 0.085	6.80 ± 0.121

Each value represents the mean ± SD ($n = 3$)

UPW ultra-pure water, *PB* phosphate buffer, *HCl* hydrochloric acid

Table 4 Droplet size, PDI, zeta potential, and viscosity of SMEDDS formulations

Formulation code	Droplet size (nm)	PDI	Zeta potential (mV)	Viscosity (cP)
F7	272.9 ± 82.7	0.415	− 57.2	5.347 ± 0.58
F8	677.8 ± 235.2	0.375	− 19.7	11.12 ± 0.77
F11	466 ± 76.3	0.538	− 3.16	10.54 ± 1.12
F12	578.9 ± 121.1	0.764	− 5.99	10.04 ± 1.09

Each value represents the mean ± SD ($n = 3$)

is a long-chain fatty acid frequently used in emulsion formulations and is the second most powerful solvent for vorinostat. While oils have the maximum capacity to solubilize drugs, solubility can be enhanced through the addition of surfactants and co-surfactants. In other studies, researchers reported that the labrasol enhanced intestinal absorption of drug exposed to high tolerance and low solubility [48, 49]. Self-microemulsification efficiency of SMEDDS formulation changes with the chain length of co-surfactant. Suppose a single surfactant film is used to facilitate the formation of self-microemulsion, the lipophilic chains of the surfactant should be sufficiently short or contain fluidizing groups (e.g., unsaturated bonds). Therefore, short-to-medium chain length (C3–C8) co-surfactants are usually added, which further reduce interfacial tension and raise the fluidity of the interface [50].

Based on solubility studies, capryol 90 and oleic acid were selected as oil phases, labrasol, and span 20 were selected as surfactants, and PEG 400 was chosen as co-surfactant for this SMEDDS development. Ultra-pure water was used as an aqueous phase. Surfactant and co-surfactant (S_{mix}) were mixed in different ratios to identify the self-microemulsion region. The self-microemulsifying region is described by colors, which is around 15% of the total area. In this study, phase diagram compositions have 20 to 40% of oil phase and more than 60% of S_{mix} concentration, which provides clear self-microemulsifying region. The efficacy of emulsion formation was good with the total concentrations of the S_{mix} over 50% of the liquid SMEDDS [51, 52].

A series of SMEDDS formulations (F1 to F12) were prepared with varying concentration of the oils (10 to 50%), surfactants (25 to 55%), and co-surfactant (17.5 to 45%). On the basis of solubility studies, the prescribed amount (~ 10 mg) of vorinostat was incorporated into the SMEDDS. These formulations were clear and moderately viscous.

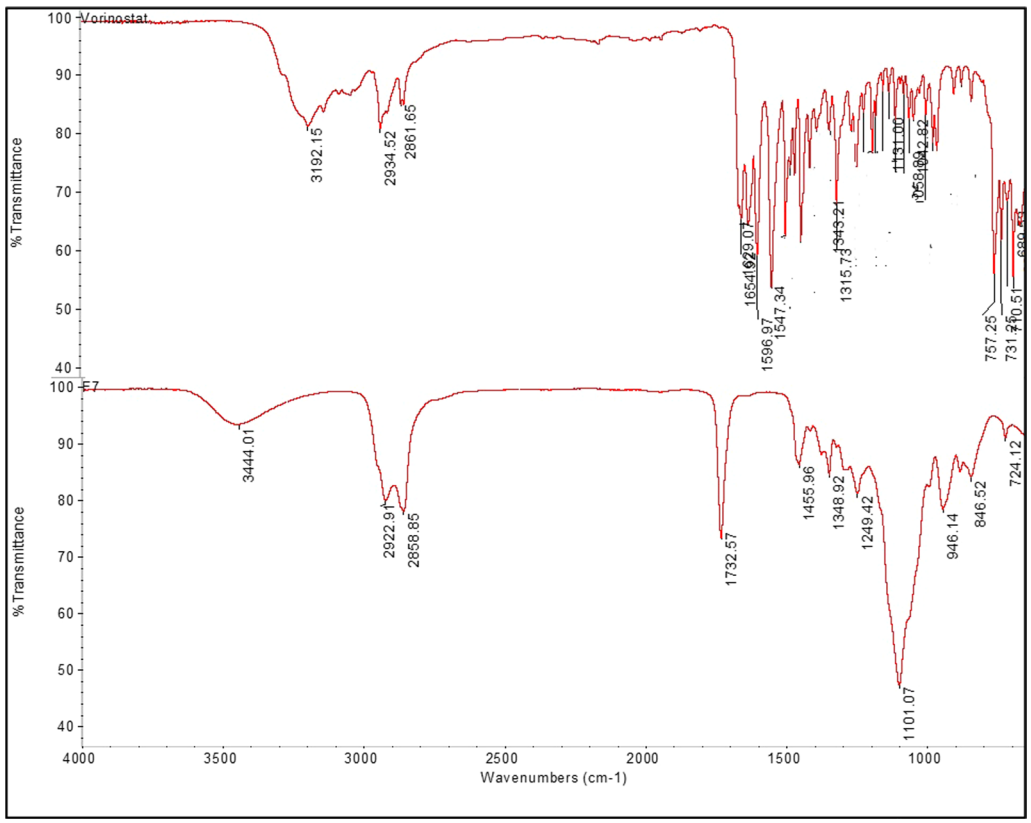

Fig. 2 FT-IR spectra of vorinostat and optimized SMEDDS formulation (F7)

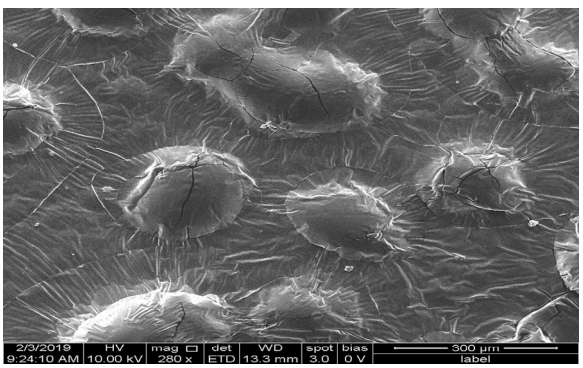

Fig. 3 Field emission scanning electron microscopy image of vorinostat-loaded self-microemulsion (F7)

Self-microemulsification time depends mainly on the individual composition and its proportion of oil, surfactant, and co-surfactant [53]. The short self-microemulsification time reported for all the investigated systems shows their ability for easy and rapid emulsification except F5, F9, and F10. Vorinostat SMEDDS formulation (F7, F8, F11, and F12) containing different ratios of capryol, labrasol, and PEG produced self-microemulsion with no phase separation, with a clear and transparent appearance, was selected for further studies.

Six different ratios of oleic acid, surfactant (labrasol), and co-surfactant (PEG 400) mixtures self-microemulsification time were investigated from 10:90 to 30:70. Excepted for the 50:50 mixture, other formulations dispersed within 3 min and produced a bluish white appearance. An increase in the concentration of surfactant was found to decrease the self-microemulsification time. In the 50:50 mixture, the concentration of labrasol was less compared to other compositions, and for this reason, no spontaneous dispersion occurred. On the other hand, the self-microemulsification time of capryol, labrasol, and PEG mixture from 20:80 to 40:60 was studied. The self-microemulsification time decreased (within 2 min) and produced a clear transparent appearance as compared to the mixture of oleic acid, labrasol, and PEG. Prepared SMEDDS formulation with increased concentration of labrasol showed spontaneity of emulsification process with minimal self-microemulsification time. This may be due to the ability of labrasol to reduce interfacial tension, causing excess diffusion of the aqueous phase into the oil, which results in significant interfacial disruption and discharge of droplets into the bulk aqueous phase.

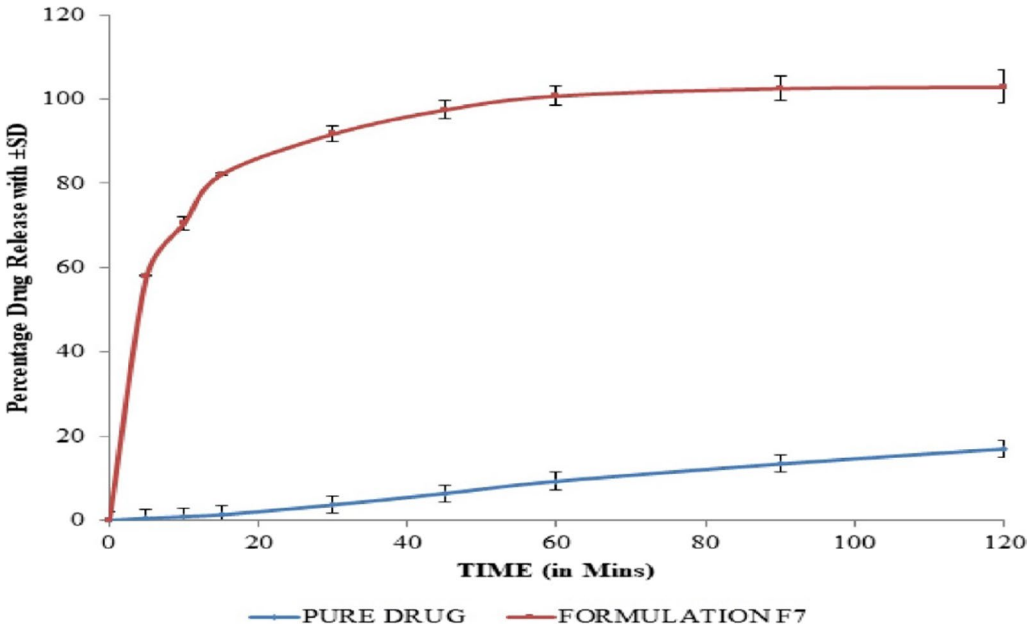

Fig. 4 Comparison of the percentage in vitro drug release between pure drug (vorinostat powder) and vorinostat-loaded optimized SMEDDS formulation (F7)

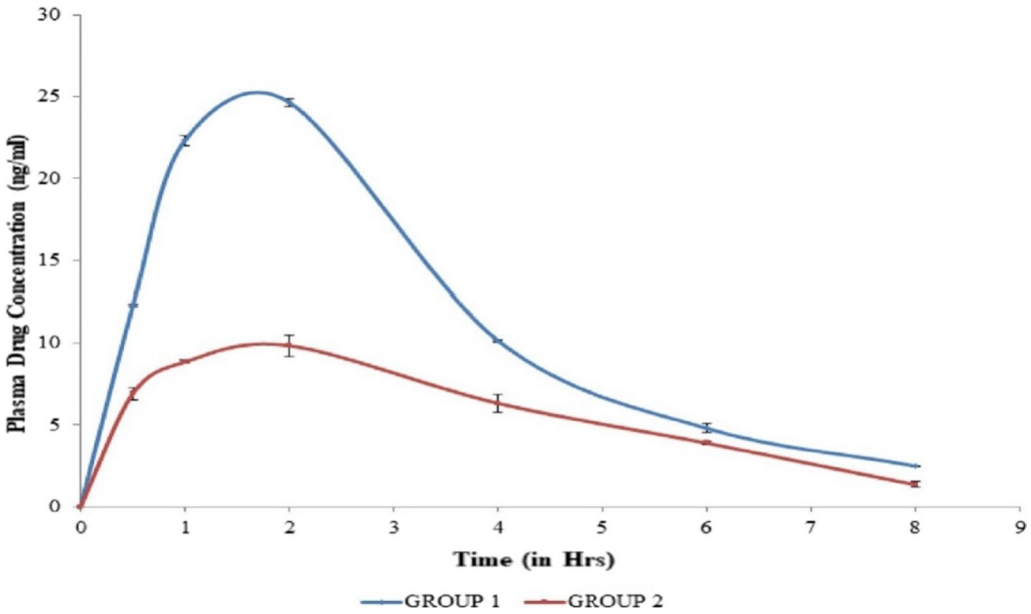

Fig. 5 Plasma concentration of vorinostat versus the time profiles of group I (SMEDDS 10 mg/kg) and group II (vorinostat in suspension 10 mg/kg)

The study revealed that the influence of labrasol and PEG 400 played a vital role along with the emulsifying properties of capryol 90 to form maximum emulsification efficiency [54]. From the above findings, the composition of capryol, labrasol, and PEG was suitable to make spontaneously dispersing and stable SMEDDS formulation for vorinostat.

The change in pH is due to the zeta potential of formulation which in turn can affect the stability of microemulsion. The selected SMEDDS formulations were exposed to different media such as ultra-pure water,

Table 5 Pharmacokinetic parameters after oral administration of vorinostat suspension (pure drug) and optimized vorinostat-loaded SMEDDS (F7)

Parameters (units)	Group I (SMEDDS 10 mg/kg)	Group II (control) API suspension 10 mg/kg)
C_{max} (ng/mL)	24.62 ± 0.28*	15.50 ± 0.29
T_{max} (h)	2.17 ± 0.02*	1.23 ± 0.09
$AUC_{(0-\infty)}$ (ng/mL h)	1325.33 ± 16.28*	365.00 ± 12.76
$t_{1/2}$ (h)	7.66 ± 0.18*	15.50 ± 0.28
$MRT_{(0-\infty)}$ (h)	11.88 ± 0.08*	22.69 ± 0.36
$F^{\#}$ (%)	363.10	–

Values are expressed as mean ± SEM of 6 animals. Symbol represents the statistical significance performed by ANOVA, followed by Tukey–Kramer's multiple comparison tests

*$p < 0.001$ indicates the comparison of group I (SMEDDS) with group II (API suspension) treated animals. Maximum plasma concentration (C_{max}). Time of maximum concentration (T_{max}), area under curve extrapolated to infinity ($AUC_{(0-\infty)}$), elimination half-life ($t_{1/2}$), mean residence time when the drug concentration profile is extrapolated to infinity ($MRT_{(0-\infty)}$), relative bioavailability ($F^{\#}$), active pharmaceutical ingredient-Vorinostat (API-Vorinostat)

0.1 M HCl, and PB pH 6.8 to mimic the in vivo conditions and revealed no signs of precipitation or phase separation, indicating that all the formulations were robust toward different pH conditions.

A dilution test was conducted by diluting prepared vorinostat-loaded SMEDDS in four different concentrations (1:50, 1:100, 1:500, and 1:1000) and three different media. After dilution of all prepared SMEDDS formulations, the resulting self-microemulsions were found to remain clear, transparent, and showed no phase separation even after 24 h, which implies the formation of stable emulsion (data not shown). This provides a good indication of the suitability of such systems for oral administration, passing along the gastrointestinal tract as emulsified oil globules without phase separation [55]. The ability of SMEDDS to be diluted without any phase separation and drug precipitation is essential for its use as a drug delivery vehicle. The freeze–thaw cycling samples were placed alternately at − 20 °C and 40 °C for 24 h at each temperature. No separation was observed in the freeze–thaw stability study, which shows that the formulations withstand different stress conditions [32].

The average droplet size of the F7 formulation is 272.9 ± 82.7 nm to 677.8 ± 235.2, which is slightly higher than reported self-microemulsifying drug delivery studies [56, 57]. The droplet size is mainly dependent on the nature and concentration of surfactant. The polydispersity values are observed from 0.375 to 0.764, which indicate that the SMEDDS droplets were almost homogenous and had narrow size distribution. The higher the value of PDI, the lower the uniformity of the droplet size. Zeta potential analysis of selected SMEDDS formulations has a negative charge (−) mV; it was in the range of − 3.16 to − 57.2 mV. In general, a zeta potential value of ± 30 mV is sufficient for stability. Except formulation F7, all other selected formulations were not stable and prone to aggregation. Zeta potential of globules was produced with a negative charge irrespective of formulation due to the anionic group of fatty acid and glycol in the emulsion composition [58]. The viscosity of the SMEDDS formulations ranged from 5.347 ± 0.58 to 11.12 ± 0.77 cP.

Previous studies confirmed that the rate and extent of drug release, absorption, and stability of a drug depend on the droplet size [59–61]. The charge of the oil droplets of SMEDDS is another property that should be assessed for increased absorption. We observed that the F7 formulation, which contains 30% of oil and 70% of surfactant and co-surfactant mixture, showed a particle size of 272.9 ± 82.7 nm (the least value among other SMEDDS formulations), and a zeta potential value of − 57.2, which was higher than other SMEDDS formulations. As a result, the F7 was chosen as an optimized formulation for further studies.

The FT-IR spectra of the optimized SMEDDS (F7) formulation showed all the characteristic peaks with minor shifts as compared to vorinostat. There was no apparent shift of bands or the emergence of new bands, confirming the absence of changes in the chemical bond formation between the drug and excipients. FESEM is mainly used to investigate the structure and morphology of microemulsions that are formed by the dilution of SMEDDS. The shape of the vorinostat-loaded self-microemulsion (F7) with capryol 90, labrasol, and PEG mixture was found to be spheroidal appearance, uniformity in droplet size with nanometer range.

The optimized SMEDDS formulation (F7) showed more than 80% are released in 15 min and neared more than 95% completion after 45 min of in vitro drug release. On the other hand, the pure drug showed 17% drug release after 120 min. Notably, SMEDDS releases the maximum percentage after 10 to 30 min. The initial burst of release might be due to the presence free drug on the surface of SMEEDS; later the drug release was found to be in a controlled manner as stated by Ameeduzzafar et al. [62]. These results revealed that the optimized SMEDDS exhibited a significantly faster release and higher dissolution percentage as compared to vorinostat powder ($p < 0.001$). The vorinostat powder showed a lower dissolution rate due to its hydrophobic nature and poor aqueous solubility. A similar finding [1] has been reported for erlotinib, which belongs to BCS class II drug. From the release kinetics, it was confirmed that the

formulation F7 obeys the Higuchi pattern, stating diffusion mediated drug release.

In in vivo pharmacokinetic studies, a significant increase in $AUC_{(0-\infty)}$ and C_{max} was observed from the SMEDDS as compared with the pure drug in suspension. $AUC_{(0-\infty)}$ and C_{max} of group I was 1325.33 ± 16.28 ng/mL h and 24.62 ± 0.28 ng/mL, respectively, and 365.00 ± 12.76 ng/mL h and 15.50 ± 0.29 ng/mL, respectively, for group II. The T_{max}, $t_{½}$ and MRT values for group I were 2.17 ± 0.02 h, 7.66 ± 0.18 h, and 11.88 ± 0.08 h, respectively, and for group II, 1.23 ± 0.09 h, 15.50 ± 0.28 h, and 22.69 ± 0.36 h, respectively. The relative bioavailability (*F*) of vorinostat SMEDDS was 363.10% (10 mg/kg) when compared to the pure drug in suspension.

In the group II, the animals treated with SMEDDS formulation (10 mg/kg, oral) exhibited a higher drug plasma concentration than vorinostat pure drug powder (10 mg/kg) at each time point. SMEDDS formulations exhibited faster absorption than the powder, which can be seen from the significant difference in plasma drug concentrations even at the 1-h time point. In the control group, vorinostat pure drug powder-treated animals (group II) exhibited the lowest average drug plasma concentration due to its low solubility and dissolution rate compared to SMEDDS formulations (group I). This result indicates that the oral bioavailability of SMEDDS 10 mg/kg (group II) was significantly ($p < 0.001$) improved when compared with the pure drug in suspension 10 mg/kg (group I). Therefore, the SMEDDS formulation of vorinostat could be effectively recognized due to the higher bioavailability and the bioavailability improvement of vorinostat SMEDDS could be interpreted in relation to absorption achieved from a larger surface area of orally administered SMEDDS [63–65].

The pharmacokinetic parameters including C_{max}, T_{max}, $AUC_{(0-\infty)}$, $t_{1/2,\ and}$ $MRT_{(0-\infty)}$ of vorinostat-loaded SMEDDS and drug powder are listed in Table 5. The optimized SMEDDS formulation (F7) 10 mg/kg (group I) showed significantly higher $AUC_{(0-\infty)}$, C_{max}, and T_{max} compared to vorinostat powder ($p < 0.01$) (group 2). Specifically, the $AUC_{(0-\infty)}$ (1325.33 ± 16.28 ng/mL h) and C_{max} (24.62 ± 0.28 ng/mL) values of SMEDDS formulation administered with 10 mg/kg were approximately 3.6-fold and 1.6-fold higher than those of vorinostat drug powder. This indicates the possibility of effective distribution of SMEDDS and microemulsification in GIT for a higher absorption rate. SMEDDS increased intestinal wall permeability through the opening of tight junctions in the intestine caused by lipids contributing to the increased permeability of poorly permeable drugs. It leads to a marked improvement in the absorption of class IV drugs [66].

Thus, vorinostat is categorized as a class IV drug by the BCS with poor aqueous solubility and permeability. Therefore, choosing appropriate pharmaceutical techniques to increase vorinostat solubility plays a key role in improving its bioavailability. In this study, we reported that SMEDDS formulation improving the solubility and bioavailability of BCS class IV drugs vorinostat to overcome both dissolution and permeability rate limited absorption.

5 Conclusions

The present study demonstrates that poorly water-soluble BCS class IV drug vorinostat with low bioavailability can be formulated as SMEDDS for improved oral bioavailability. The optimized SMEDDS of vorinostat was thermodynamically stable with good self-microemulsification efficiency. The optimized formulation (F7) particle size was found to be 272.9 ± 82.7, with a PDI of 0.415, and zeta potential of − 57.2 mV. The in vitro dissolution of vorinostat-loaded SMEDDS (F7) was 6.0-fold higher than pure vorinostat, and in vivo pharmacokinetic showed significant improvement in the extent of absorption of vorinostat in rats. The optimized formulation has shown C_{max} 1.6-fold and $AUC_{(0-\infty)}$ 3.6-fold of greater bioavailability than a drug in suspension. It can be concluded that the present exploratory study has successfully illustrated the potential utility of SMEDDS for the delivery of hydrophobic compound vorinostat. Due to its ease of manufacture, scalability, and physical stability, the developed liquid/semisolid SMEDDS formulation can be employed in the future to address the solubility issue of poorly water-soluble drugs.

Abbreviations

$AUC_{(0-\infty)}$: Area under the plasma drug concentration–time curve; BCS: Biopharmaceutical classification system; C_{max}: Maximum plasma drug concentration; FESEM: Field emission scanning electron microscopy; FT-IR: Fourier-transform infrared; GI: Gastrointestinal; GIT: Gastrointestinal tract; HDAC: Histone deacetylase; HPLC: High-performance liquid chromatography; PB: Phosphate buffer; PBS: Phosphate-buffered solution; PDI: Polydispersity index; PEG: Polyethylene glycol; SD: Standard deviation; SMEDDSs: Self-microemulsifying drug delivery systems; $t_{1/2}$: Elimination half-life; T_{max}: Time to reach the maximum plasma drug concentration.

Supplementary Information

The online version contains supplementary material available at https://doi.org/10.1186/s43088-022-00279-z.

Additional file 1. Pseudoternary phase diagram of series1: Oleic acid, labrasol and PEG 400 (Smix 1:1, 3:1), series 2: Capryol 90, labrasol and PEG 400 (Smix 2:1, 3:1), series 3: Capryol 90, span 20 and PEG 400 (Smix 1:1, 3:1).

Additional file 2. Particle size distribution and PDI of vorinostat loaded SMEDDS (F7).

Additional file 3. Zetapotential of vorinostat loaded SMEDDS (F7).

Additional file 4. FT-IR spectra of vorinostat with capryol 90, labrasol and PEG 400.

Acknowledgements
This work was financially supported by Pioneer Scientists Incentive Fund (Proj-In-FPS-015) from Centre of Excellence in Research Value Innovation and Entrepreneurship (CERVIE), UCSI University, Malaysia. The authors would like to thank Faculty of Pharmaceutical Sciences, UCSI University, Cheras, Malaysia and KPJ Healthcare University College, Nilai, Malaysia, for providing necessary facilities to carry out this work.

Author contributions
AKJ designed the self-microemulsifying drug delivery system studies for vorinostat, contributed to construction of pseudoternary phase diagram, participated in the sequence alignment, and drafted the manuscript. TI carried out the vorinostat solubility study and prepared and characterized the vorinostat self-micro-emulsion. LKB participated in the HPLC analysis and in vitro drug release studies and performed the statistical analysis. ME carried out the in vivo pharmacokinetic studies. HSJC conceived of the animal study and participated in its design and coordination and helped to draft the manuscript. All authors read and approved the final manuscript.

Funding
This study was supported by Pioneer Scientists Incentive Fund (PSIF), Project code: Proj-In-FPS-015, from Centre of Excellence in Research Value Innovation and Entrepreneurship (CERVIE), UCSI University, Malaysia, and procured the active pharmaceutical ingredients, standards, excipients, chemicals, and reagents through CERVIE, UCSI University.

Availability of data and materials
All data generated or analyzed during this study are included in this published article.

Declarations

Ethics approval and consent to participate
All animal experiments and the procedures involving were adhered to standard protocol complying with the European Union guidelines (directive 2010/63/EU) followed by institutional animal ethics committee (IAEC), KPJ Healthcare University College, Nilai, Malaysia. The experimental protocol was approved, and consent for animal experimentation was obtained from IAEC (Ref. No. KPJUC/RMC/EC/2018/132).

Consent for publication
Not applicable.

Competing interests
The authors declare that there are no competing interests. The authors alone are responsible for the content and writing of this article.

Author details
[1]Faculty of Pharmaceutical Sciences, UCSI University, 56000 Cheras, Kuala Lumpur, Malaysia. [2]Faculty of Pharmacy, University of Cyberjaya, Persiaran Bestari, 63000 Cyberjaya, Selangor, Malaysia. [3]Department of Pharmacology and Chemistry, Faculty of Pharmacy, Universiti Teknologi MARA, 42300, Puncak Alam, Selangor, Malaysia.

Received: 23 July 2021 Accepted: 25 July 2022
Published online: 13 August 2022

References

1. Truong DH, TranTH RT, Choi JY, Lee HH, Moon C, Kim JO (2016) Development of solid self-emulsifying formulation for improving the oral bioavailability of erlotinib. AAPS PharmSciTech 17(2):466–473
2. Kavitha A, Janakiraman K, Dang R (2021) Quality by design based development of etravirine self micro emulsifying drug delivery system. Int J Appl Pharm 13:103–111
3. Akiladevi D, Kumar SS (2019) Formulation development and evaluation of self-nanoemulsifiedliquisolid compacts of a poorly soluble biopharmaceutics classification system Class II drug. Drug Invention Today 11(11):2854–2858
4. Gao H, Jia H, Dong J, Yang X, Li H, Ouyang D (2021) Integrated in silico formulation design of self-emulsifying drug delivery systems. Acta Pharm Sin B. https://doi.org/10.1016/j.apsb.2021.04.017
5. Akhtar N, Mohammed SA, Khan RA, Yusuf M, Singh V, Mohammed HA, Khadri H (2020) Self-generating nano-emulsification techniques for alternatively routed, bioavailability enhanced delivery, especially for anti-cancers, anti-diabetics, and miscellaneous drugs of natural, and synthetic origins. J Drug Deliv Sci Technol 58:101808
6. Wadhwa J, Nair A, Kumria R (2012) Emulsion forming drug delivery system for lipophilic drugs. Acta Pol Pharm 69(2):179–191
7. Krishnamoorthy B, Rahman SH, Rajkumar M, Vamshikrishna K, Gregory M, Vijayaraghavan C (2015) Design, formulation, in vitro, in vivo, and pharmacokinetic evaluation of nisoldipine-loaded self-nanoemulsifying drug delivery system. J Nanopart Res 17(1):1–11
8. Zhang Y, He L, Yue S, Huang Q, Zhang Y, Yang J (2017) Characterization and evaluation of a self-microemulsifying drug delivery system containing tectorigenin, an isoflavone with low aqueous solubility and poor permeability. Drug Deliv 24(1):632–640
9. Kale SN, Deore SL (2017) Emulsion micro emulsion and nano emulsion: a review. Syst Rev Pharm 8(1):39
10. Olsen EA, Kim YH, Kuzel TM, Pacheco TR, Foss FM, Parker S, Duvic M (2007) Phase IIb multicenter trial of vorinostat in patients with persistent, progressive, or treatment refractory cutaneous T-cell lymphoma. J Clin Oncol 25(21):3109–3115
11. Cai YY, Yap CW, Wang Z, Ho PC, Chan SY, Ng KY, Lin HS (2010) Solubilization of vorinostat by cyclodextrins. J Clin Pharm Ther 35(5):521–526
12. Verma R, Kaushik D (2020) Design and optimization of candesartan loaded self-nanoemulsifying drug delivery system for improving its dissolution rate and pharmacodynamic potential. Drug Deliv 27(1):756–771
13. Marks PA (2007) Discovery and development of SAHA as an anticancer agent. Oncogene 26(9):1351–1356
14. Kavanaugh SA, White LA, Kolesar JM (2010) Vorinostat: a novel therapy for the treatment of cutaneous T-cell lymphoma. Am J Health Syst Pharm 67(10):793–797
15. Sandhu P, Andrews PA, Baker MP, Koeplinger KA, Soli ED, Miller T, Baillie TA (2007) Disposition of vorinostat, a novel histone deacetylase inhibitor and anticancer agent, in preclinical species. Drug Metab Lett 1(2):153–161
16. Venkatesh PR, Goh E, Zeng P, New LS, Xin L, Pasha MK, Sangthongpitag K, Yeo P, Kantharaj E (2007) In vitro phase I cytochrome P450 metabolism, permeability and pharmacokinetics of SB639, a novel histone deacetylase inhibitor in preclinical species. Biol Pharm Bull 30(5):1021–1024
17. Konsoula R, Jung M (2008) In vitro plasma stability, permeability and solubility of mercaptoacetamide histone deacetylase inhibitors. Int J Pharm 361(1–2):19–25
18. Du L, Musson DG, Wang AQ (2005) High turbulence liquid chromatography online extraction and tandem mass spectrometry for the simultaneous determination of suberoylanilide hydroxamic acid and its two metabolites in human serum. Rapid Commun Mass Spectrom 19(13):1779–1787
19. Tran TH, Chu DT, Truong DH, Tak JW, Jeong JH, Hoang VL, Yong CS, Kim JO (2016) Development of lipid nanoparticles for a histone deacetylases inhibitor as a promising anticancer therapeutic. Drug Deliv 23(4):1335–1343
20. Dai W, Wang C, Yu C, Yao J, Sun F, Teng L, Li Y (2015) Preparation of a mixed-matrix hydrogel of vorinostat for topical administration on the rats as experimental model. Eur J Pharm Sci Off J Eur Fed Pharm Sci 78:255–263
21. Tran TH, RamasamyT TDH, Shin BS, Choi HG, Yong CS, Kim JO (2014) Development of vorinostat-loaded solid lipid nanoparticles to enhance pharmacokinetics and efficacy against multidrug-resistant cancer cells. Pharm Res 31(8):1978–1988. https://doi.org/10.1007/s11095-014-1300-z
22. Prajapat MD, Patel NJ, Bariya A, Patel SS, Butani SB (2017) Formulation and evaluation of self-emulsifying drug delivery system for nimodipine, a BCS class II drug. J Drug Deliv Sci Technol 39:59–68
23. Silva AE, Barratt G, Chéron M, Egito EST (2013) Development of oil-in-water microemulsions for the oral delivery of amphotericin B. Int J Pharm 454(2):641–648
24. Zhu JX, Tang D, Feng L, Zheng ZG, Wang RS, Wu AG, Zhu Q (2013) Development of self-microemulsifying drug delivery system for oral bioavailability enhancement of berberine hydrochloride. Drug Dev Ind Pharm 39(3):499–506

25. Yin YM, Cui FD, Mu CF, Choi MK, Kim JS, Chung SJ, Kim DD (2009) Docetaxel microemulsion for enhanced oral bioavailability: preparation and in vitro and in vivo evaluation. J Control Release 140(2):86–94
26. Ahmad J, Mir SR, Kohli K, Chuttani K, Mishra AK, Panda AK, Amin S (2014) Solid-nanoemulsion preconcentrate for oral delivery of paclitaxel: formulation design, biodistribution, and γ scintigraphy imaging. BioMed Res Int 2014:984756
27. Chouhan P, Saini TR (2016) D-optimal design and development of microemulsion based transungual drug delivery formulation of ciclopirox olamine for treatment of onychomycosis. Indian J Pharm Sci 78(4):498–511
28. Laddha P, Suthar V, Butani S (2014) Development and optimization of self microemulsifying drug delivery of domperidone. Braz J Pharm Sci 50(1):91–100
29. Katla VM, Veerabrahma K (2016) Cationic solid self-micro emulsifying drug delivery system (SSMED) of losartan: formulation development, characterization, and in vivo evaluation. J Drug Deliv Sci Technol 35:190–199
30. Jakki R, Syed MA, Kandadi P, Veerabrahma K (2013) Development of a self-microemulsifying drug delivery system of domperidone: in vitro and in vivo characterization. Acta Pharm 63(2):241–251
31. Patel J, Kevin G, Patel A, Raval M, Sheth N (2011) Design and development of a self-nanoemulsifying drug delivery system for telmisartan for oral drug delivery. Int J Pharm Investig 1(2):112–118
32. Chandrasekaran N (2015) Nanoemulsion formation and characterization by spontaneous emulsification: investigation of its antibacterial effects on Listeria monocytogenes. Asian J Pharm 9(1):23–28
33. Morsi NM, Mohamed MI, Refai H, El Sorogy HM (2014) Nanoemulsion as a novel ophthalmic delivery system for acetazolamide. Int J Pharm Pharm Sci 6(14):227–236
34. Morsi N, Ibrahim M, Refai H, El Sorogy H (2017) Nanoemulsion-based electrolyte triggered in situ gel for ocular delivery of acetazolamide. Eur J Pharm Sci 104:302–314
35. Amanda Ng TW, Ashok Kumar J, Liew KB, Melbha S, Habibur Rahman E (2019) The effects of the combination of biodegradable and synthetic polymers on the release behaviour of Nateglinide matrix tablets. J Excip Food Chem 10(1):13–22
36. Shah RM, Eldridge DS, Palombo EA, Harding IH (2016) Encapsulation of clotrimazole into solid lipid nanoparticles by microwave-assisted microemulsion technique. Appl Mater Today 5:118–127
37. Kim GG, Poudel BK, Marasini N, Lee DW, Hiep TT, Yang KY, Choi HG (2013) Enhancement of oral bioavailability of fenofibrate by solid self-microemulsifying drug delivery systems. Drug Dev Ind Pharm 39(9):1431–1438
38. Tao C, Wen X, Zhang Q, Song H (2019) Solid sirolimus self-microemulsifying drug delivery system: development and evaluation of tablets with sustained release property. Iran J Pharm Res 18(4):1648
39. Javier G, Jan BP, Bryan H, Anne DD, Marcel G. The European Framework on Research Animal Welfare Regulations and Guidelines. In: Guillén J, editor. Laboratory animals, 2nd edn. London: Academic Press; 2018. p. 117–202. ISBN 9780128498804. https://doi.org/10.1016/B978-0-12-849880-4.00005-2.
40. Jangipuria FO, Londhe VA (2015) Solubility enhancement of lurasidone hydrochloride by preparing SMEDDS. Int J Pharm Pharm Sci 7(11):283–288
41. Charan J, Kantharia N (2013) How to calculate sample size in animal studies? J Pharmacol Pharmacother 4:303–306. https://doi.org/10.4103/0976-500X.119726
42. Mahmoudian M, Valizadeh H, Löbenberg R, Zakeri-Milani P (2020) Enhancement of the intestinal absorption of bortezomib by self-nanoemulsifying drug delivery system. Pharm Dev Technol 25(3):351–358
43. Wayne RT (2003) Chemical safety in animal care, use, and research. ILAR J 44(1):13–19
44. Nepal PR, Han HK, Choi HK (2010) Preparation and in vitro–in vivo evaluation of Witepsol® H35 based self-nanoemulsifying drug delivery systems (SNEDDS) of coenzyme Q10. Eur J Pharm Sci 39(4):224–232
45. Fritz HF, Ortiz AC, Velaga SP, Morales JO (2018) Preparation of a novel lipid-core micelle using a low-energy emulsification method. Drug Deliv Transl Res 8(6):1807–1814
46. Balakrishnan P, Lee BJ, Oh DH, Kim JO, Hong MJ, Jee JP, Choi HG (2009) Enhanced oral bioavailability of dexibuprofen by a novel solid self-emulsifying drug delivery system (SEDDS). Eur J Pharm Biopharm 72(3):539–545
47. Lou H, Qiu N, Crill C, Helms R, Almoazen H (2013) Development of w/o microemulsion for transdermal delivery of iodide ions. AAPS PharmSciTech 14(1):168–176
48. Hu Z, Tawa R, Konishi T, Shibata N, Takada K (2001) A novel emulsifier, labrasol, enhances gastrointestinal absorption of gentamicin. Life Sci 69(24):2899–2910
49. Piao HM, Balakrishnan P, Cho HJ, Kim H, Kim YS, Chung SJ, Kim DD (2010) Preparation and evaluation of fexofenadine microemulsions for intranasal delivery. Int J Pharm 395(1–2):309–316
50. Muzaffar FA, Singh UK, Chauhan L (2013) Review on microemulsion as futuristic drug delivery. Int J Pharm Pharm Sci 5(3):39–53
51. Czajkowska-Kośnik A, Szekalska M, Amelian A, Szymańska E, Winnicka K (2015) Development and evaluation of liquid and solid self-emulsifying drug delivery systems for atorvastatin. Molecules 20(12):21010–21022
52. Singh D, Tiwary AK, Bedi N (2019) Self-microemulsifying drug delivery system for problematic molecules: an update. Recent Pat Nanotechnol 13(2):92–113
53. Kallakunta VR, Bandari S, Jukanti R, Veerareddy PR (2012) Oral self emulsifying powder of lercanidipine hydrochloride: formulation and evaluation. Powder Technol 221:375–382
54. Oza N, Sagar S, Khodakiya A (2020) Use of simplex lattice design in development of oral self-nanoemulsifying drug delivery system containing rosuvastatin calcium. Int J Appl Pharm 12(3):40–47
55. Pol AS, Patel PA, Hegde D (2013) Peppermint oil-based drug delivery system of aceclofenac with improved anti-inflammatory activity and reduced ulcerogenecity. Int J Pharm Biosci Technol 1(2):89–101
56. Katla VM, Veerabrahma K (2016) Cationic solid self micro emulsifying drug delivery system (SSMED) of losartan: formulation development, characterization and in vivo evaluation. J Drug Deliv Sci Technol 35:190–199. https://doi.org/10.1016/j.jddst.2016.04.011
57. Dangre P, Gilhotra R, Dhole S (2016) Formulation and statistical optimization of self-microemulsifying drug delivery system of eprosartan mesylate for improvement of oral bioavailability. Drug DelivTransl Res 6(5):610–621. https://doi.org/10.1007/s13346-016-0318-7
58. Madan JR, Sudarshan B, Kadam VS, Kama D (2014) Formulation and development of self-microemulsifying drug delivery system of pioglitazone. Asian J Pharm 8(1):1–8
59. Sabale V, Vora S (2012) Formulation and evaluation of microemulsion-based hydrogel for topical delivery. Int J Pharm Investig 2(3):140–149
60. Chaitali J, Vaishali K, Santosh P (2015) Formulation and evaluation of antifungal non-aqueous microemulsion for topical drug delivery of griseofulvin. Inventi Impact Pharm Tech 1:38–50
61. Dokania S, Joshi AK (2015) Self-microemulsifying drug delivery system (SMEDDS)—challenges and road ahead. Drug Deliv 22(6):675–690
62. Ameeduzzafar Z, Syed SI, Alruwaili NK, Omar AA, Mohammed HE, Mohammed MG, Sultan A, Ahmed Mahmoud AA, Khalid SA, Mohd Y, Kaveripakkam MN, Sami IA, Abdullah SA (2021) Development of piperine-loaded solid self-nanoemulsifying drug delivery system: optimization, in vitro, ex vivo, and in vivo evaluation. Nanomaterials (Basel) 11(11):2920
63. Wu L, Qiao Y, Wang L, Guo J, Wang G, He W, Zhao J (2015) A self-microemulsifying drug delivery system (SMEDDS) for a novel medicative compound against depression: a preparation and bioavailability study in rats. AAPS PharmSciTech 16(5):1051–1058
64. Mohamed EA, Hashim A II, Yusif RM, Suddek GM, Shaaban AAA, Badria FAE (2017) Enhanced in vitro cytotoxicity and anti-tumor activity of vorinostat-loaded pluronic micelles with prolonged release and reduced hepatic and renal toxicities. Eur J Pharm Sci 96:232–242
65. Yan B, Ma Y, Guo J, Wang Y (2020) Self-microemulsifying delivery system for improving bioavailability of water insoluble drugs. J Nanopart Res 22(1):1–14
66. Akula S, Gurram AK, Devireddy SR (2014) Self-microemulsifying drug delivery systems: an attractive strategy for enhanced therapeutic profile. Int Sch Res Not 2014:964051. https://doi.org/10.1155/2014/964051

Publisher's Note